

NASA  
TP  
1013  
c.1

NASA Technical Paper 1013 c.1

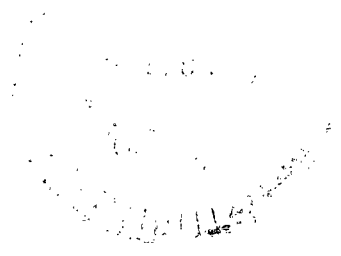
TECH LIBRARY KAFB, NM  
0134315

LOAN COPY: 1  
AFWL TECHNIC.  
KIRTLAND AFB, N. M.

# Measurements of the Tonal Component of Cavity Noise and Comparison With Theory

P. J. W. Block

NOVEMBER 1977





NASA Technical Paper 1013

# Measurements of the Tonal Component of Cavity Noise and Comparison With Theory

P. J. W. Block  
Langley Research Center  
Hampton, Virginia

**NASA**

National Aeronautics  
and Space Administration

**Scientific and Technical  
Information Office**

1977

## SUMMARY

This paper presents the results of a detailed study of the frequency of the tonal noise generated by a flow-excited rectangular cavity. The Mach number in this experimental study ranged from 0.05 to 0.40, and the cavity length-to-depth ratio varied from 0.1 to 8. The data are used to evaluate a current prediction method and good agreement is shown. Measurements of the minimum streamwise cavity length required for oscillation were also made.

## INTRODUCTION

Noise produced by flow-excited cavities has been shown to be an important contributor to the overall nonpropulsive or airframe noise of an aircraft on approach to an airport. This noise has both broadband and tonal components, with the latter being the more annoying element of the overall noise. As yet, no reliable method exists for predicting either component of the noise produced.

In 1975, Block and Heller (ref. 1) reported the first farfield measurements of the noise produced by rectangular-shaped flow-excited cavities. Subsequently, much research has been focused on determining the mechanisms responsible for such generation of sound and on predicting the oscillation frequency of the tonal component of the noise. In particular, previous studies of the large-scale pressure oscillations found inside flow-excited cavities (see ref. 1 for review of this literature) have aided in describing the flow structures in and around the cavity.

In 1964, Rossiter (ref. 2) developed a semiempirical relationship for the Strouhal number  $N_{Str}$  of the large-scale pressure oscillations measured inside cavities. His formula, which showed a dependence of  $N_{Str}$  on the Mach number  $M$  and length-to-depth ratio  $l/d$ , gave fair agreement with the data he obtained. However, more recent data (ref. 3) show a variation of  $N_{Str}$  with  $l/d$  in a manner opposite to that indicated by Rossiter's formula. Subsequently, Block (ref. 3) attempted to include the effect of  $l/d$  on  $N_{Str}$  with an extension of the analytical approach used by Bilanin and Covert (ref. 4). This extension yielded a formula which gave fair agreement with available data. It also yielded the same variation of  $N_{Str}$  with  $l/d$  as shown by available data. However, a detailed set of experimental data was needed to test the formula developed by Block. This need provided the motivation for the present work.

Of further interest in the cavity-oscillation problem is the minimum cavity (streamwise) length that is necessary for cavity oscillation. Krishnamurty Karamcheti (ref. 5), who noted that there was some minimum cavity length below which no oscillations were observed, also noted that this minimum length  $l_{\min}$  was dependent on the velocity. This dependence, however, has not been investigated for subsonic Mach numbers.

In order to test adequately the range of validity of the equation obtained by Block (ref. 3), a parametric study (varying  $l/d$  and  $M$ ) of the frequency of cavity oscillation was necessary. This study was performed in three phases. In the first phase,  $l/d$  was fixed and the Mach number varied. In the second phase, the Mach number was fixed and the  $l/d$  ratio varied. The Mach number ranged from 0.05 to 0.40, and the cavity  $l/d$  varied from about 0.1 to 8. The final phase of this study investigated  $l_{\min}$  as a function of the Mach number over the aforementioned subsonic range.

#### SYMBOLS

A, B	empirical constants in equation (2)
c	speed of sound
d	cavity depth
f	frequency, kHz
$k_v$	ratio of average vortex convection velocity across cavity length to free-stream velocity
$l$	cavity length (streamwise direction)
$l_{\min}$	minimum streamwise cavity length required for oscillation
M	Mach number
$N_{\text{Str}}$	Strouhal number, $fl/U$
n	mode number of lengthwise cavity oscillation
U	free-stream velocity
w	cavity width

## EXPERIMENTAL ARRANGEMENT AND PROCEDURE

### Apparatus

The cavity used in this experiment was designed to have a continuously variable streamwise length (0 to 30 cm) and a depth which varied in two steps, 3.19 cm and 5.11 cm. The latter was accomplished by sliding blocks as shown in figure 1. The cavity was 5.08 cm wide (cross-stream dimension).

The apparatus was constructed of tempered, 1.25-cm-thick, aluminum barstock. The cavity was set in a 1.25-cm-thick, tempered, aluminum plate which was curved downstream of the cavity to reduce any trailing-edge noise. (See fig. 2.) The plate was flush with the lower lip of a 30-cm by 45-cm nozzle. The nozzle exit velocity varied from a Mach number of 0.05 to 0.40. The maximum shear layer thickness at the cavity leading edge was approximately 0.8 cm, and the average convection velocity across the cavity mouth was about  $0.6U$  so that  $k_v = 0.6$ . The experiment was performed in the open-jet acoustic flow facility at the Langley aircraft noise reduction laboratory (ANRL). This facility is described in reference 6.

### Acoustic Data

The acoustic data were obtained with a 1/2-inch condenser-type microphone. The data-acquisition system consisted of a preamplifier, power supply, filter, amplifier, and spectrum analyzer. The spectrum analyzer was capable of identifying the frequency of the tones in the radiated noise spectrum of the cavity to within  $\pm 0.01$  kHz. This allowed sufficiently accurate determination of the frequency which was used to calculate the Strouhal number ( $N_{Str} = fl/U$ ). The microphone was located 2.13 m above the cavity as indicated in figure 2. Initial surveys of the directivity of the noise generated by the cavity showed no strongly directional radiation patterns for any of the cases tested herein. In fact, the peak of the generally broad radiation pattern was above the cavity where the microphone was located for this entire test.

### Procedure

The test was conducted in three phases. The first phase yielded the Strouhal number as a function of Mach number. Here, the cavity dimensions were fixed, thus yielding a particular value of  $l/d$ . The five sets of cavity dimensions used in this phase of the experiment are listed in table I. The three values of  $l/d$  were 0.78 for a fairly deep cavity, 5.01 for a relatively shallow cavity, and 2.35 as an intermediate value. After the  $l/d$  value was set, the Mach number was varied in small (0.01) increments from  $M = 0.05$  to 0.40 and the frequency of the radiated tones was recorded. At times, the noise spectrum recorded by the on-line spectrum analyzer revealed several tones,

some of which were harmonically related. Each frequency was recorded for the purpose of calculating the Strouhal number. The cavity dimensions were then adjusted to give the same value of  $l/d$  and the process was repeated. About 300 data points were recorded in this phase.

In the second phase of this experiment, the dependence of the Strouhal number on the length-to-depth ratio  $l/d$  was investigated. The cavity length was varied in small increments while the Mach number remained fixed. This was done at both cavity depths (3.19 cm and 5.11 cm). The length varied from 0 to 30 cm. The two Mach numbers were 0.22 and 0.35.

The last phase was designed to determine the minimum length required for oscillation as a function of Mach number (in the lower subsonic range). To do this, the cavity was closed ( $l = 0$ ) and the Mach number was set. Then, the streamwise length  $l$  was slowly increased until oscillation commenced. This cavity length and frequency of oscillation were recorded. The Mach number was increased from 0.08 to 0.39 in 0.01 increments. These measurements were made at both cavity depths.

## RESULTS

The primary results of this experiment yielded the nondimensional frequency or Strouhal number of the cavity tones as a function of Mach number and  $l/d$ . The Strouhal number is computed from the data as  $N_{Str} = fl/U$  where  $f$  is the frequency of the cavity oscillation measured in the farfield by the microphone,  $l$  is the streamwise cavity length, and  $U$  is the free-stream velocity.

### Strouhal Number as a Function of Mach Number

The Strouhal numbers of all the data obtained in the first phase of this experiment are shown in figure 3 along with the prediction given by Block (ref. 3). This prediction will be discussed subsequently. The data for the same value of  $l/d$  is represented by the same symbol, as listed in the key. The data with  $l/d = 0.78$  are represented by circles, with the closed circles representing the cavity with smaller dimensions but the same  $l/d$  ratio. The squares represent data with  $l/d = 2.35$ , and the triangles represent data with  $l/d = 5.01$ .

Figure 3 shows that the data, which were obtained at 0.01 increments in the Mach number, lie in bands. The existence of several bands over the same Mach number range for a given cavity indicates that several frequencies are radiated from the cavity simultaneously. These frequencies may be harmonically related (for example,  $l/d = 0.78$  where  $0.3 < M < 0.4$ ) or nonharmonically related (for example,  $l/d = 0.78$

where  $0.2 < M < 0.25$ ). Thus, they may possibly be generated by two different sources or mechanisms.

The bands formed by the data are almost horizontal at the higher Mach numbers. As  $M$  decreases, data bands with a steeper slope are predominant. The steeper slopes are observed for  $M \lesssim 0.20$ . Generally, it can be seen that data points with the same value of  $l/d$  lie close to each other and form bands of similar shape. At a given Mach number, data with a larger value of  $l/d$  have a slightly larger value of  $N_{Str}$ , indicating that  $l/d$  is an important parameter.

Having observed the trends in the data, these results can also be compared with the prediction given by Block (ref. 3):

$$N_{Str} = \frac{n}{\frac{1}{k_v} + M\left(1 + \frac{0.514}{l/d}\right)} \quad (1)$$

Equation (1) predicts the Strouhal numbers of favored lengthwise cavity oscillations which can be produced by a vortical-acoustic feedback mechanism. It is based on the following physical model. Vortices which are shed periodically from the cavity leading edge travel downstream in the shear layer and react with the trailing edge to generate periodic pressure or sound pulses. These sound pulses travel upstream (subsonic flows) and disturb the shear layer which is forming at the leading edge. This disturbance triggers the formation of vortices at the leading edge and the feedback loop is completed. These lengthwise oscillations are predominant for shallower cavities (i.e.,  $l/d \gtrsim 1$ ) and, thus, equation (1) is considered most appropriate for this  $l/d$  range.

A version of equation (1) modified for deeper cavities is presented in appendix A. This modified version emphasizes the effect at the leading edge of the sound pulses which are reflected from the bottom surface of the cavity. It is more appropriate for deeper cavities ( $l/d \lesssim 1$ ); however, it is not compared with the data presented in figure 3 (e.g.,  $l/d = 0.78$ ). Instead, it is compared with the data presented in appendix B. Appendix B contains the measured raw data from phases 1 (frequency against Mach number) and 2 (frequency against cavity length). It is provided for those interested in comparing these experimental results with other results or theories. Also, for the convenience of the reader, equation (1) and the modification for deeper cavities are presented therein.

Equation (1) is a function of  $l/d$  and is plotted for the three values of  $l/d$  appropriate to the data in figure 3. It is also a function of  $n$ , the mode or stage number, and is plotted for the first six values of  $n$ . The mode number  $n$  and the  $l/d$  ratio of each of the curves in figure 3 is given to the left and right of the curves, respectively.

For the  $n = 1$  curve, the single-prediction curve for  $l/d = 0.78$  is plotted since only data of this value of  $l/d$  appear in this range of Strouhal number. An explanation for this phenomenon will be offered subsequently. (Although it is not always unambiguous to which mode a given bit of data should be ascribed, the concept of oscillation in a particular mode here implies data which lie reasonably close to the prediction of equation (1) for that particular mode or stage number  $n$ .)

Figure 3 shows that for  $M \gtrsim 0.2$  and  $l/d \gtrsim 1$ , equation (1) predicts the Strouhal numbers of the data. That is, equation (1) compares well with the behavior of the horizontal bands of data. It also correctly predicts the increase in  $N_{Str}$  when  $l/d$  increases. This aspect is further investigated in phase 2 of the experiment.

At Mach numbers below about 0.2, the data tend to deviate from the horizontal bands, and the prediction of equation (1), in favor of bands of steeper slope which are not predicted by equation (1). This transition to a steeper slope at lower Mach numbers was also observed in reference 3, particularly for deeper cavities.

It was found by East (ref. 7) that the Strouhal number of deeper cavities ( $l/d \lesssim 2$ ) at low Mach number tend to be described by a depthwise standing-wave oscillation and follow an equation of the form given by Rayleigh. The equation is

$$N_{Str} = \frac{1}{M} \left( \frac{l}{d} \right)^{1/4} \frac{1}{1 + A \left( \frac{l}{d} \right)^B} \quad (2)$$

where  $A$  and  $B$  are empirical constants having values of 0.65 and 0.75, respectively, and are based on the data reported in reference 7. Equation (2) is a representation of the Strouhal number for deeper cavities that are oscillating in the first depthwise standing-wave mode. It can be compared with the data in a manner similar to equation (1). This comparison is shown in figure 4. The dashed-line curves represent equation (2) for  $l/d = 0.78$  and 2.35. Equation (2) is not appropriate for the shallowest cavity of  $l/d = 5.01$ .

Figure 4 shows that the dashed-line curves, representing equation (2), have the characteristic behavior of increasing slope as the Mach number decreases. This was anticipated from the form of equation (2) because of the factor  $1/M$ . Although equation (2) does not accurately predict the Strouhal number at these lower Mach numbers, it does predict the trend of the data. This tends to indicate that at the lower Mach numbers ( $0.05 < M < 0.15$ ) the predominant cavity noise mechanism could be a depthwise standing-wave oscillation or, perhaps, a Helmholtz type of oscillation which would have a Strouhal relationship similar to equation (2). There is apparently a gradual transition between the two different mechanisms which occurs between  $M = 0.15$  and  $0.25$  for the cavities tested.



Finally, a rough relationship appears to exist between the intersection of the dashed- and solid-line curves representing the two different types of oscillation and the Mach number at which oscillation begins to occur in a given mode. For example, as can be seen in figure 4, in mode 1 ( $n = 1$ ), oscillation begins at about  $M = 0.23$ , and the intersection occurs at  $M = 0.26$  for data with  $l/d = 0.78$ . In mode 2 ( $n = 2$ ), oscillation begins at  $M = 0.11$  for data with  $l/d = 0.78$ , and the intersection of the  $l/d = 0.78$  lines is at  $M = 0.11$ . However, in mode 2, oscillations for the cavity having  $l/d = 2.35$  commence at  $M = 0.16$  while the intersection does not occur until  $M = 0.25$ . Also of note is the fact that no oscillations for  $l/d = 2.35$  are found in mode 1. It is believed that oscillations will begin at this value of  $l/d$  in mode 1, but at a Mach number exceeding the range used in this experiment. That is, for example, the oscillations will occur at a Mach number corresponding to the intersection of the  $l/d = 2.35$  lines of equations (1) and (2) in mode 1. This occurs around  $M = 0.65$ . This value of  $M$  is obtained by setting equation (1) equal to equation (2) and solving for  $M$ ; thus,

$$M = \frac{\frac{1}{k_v} \frac{l}{d}}{4n \left[ 1 + A \left( \frac{l}{d} \right)^B \right] - \left( \frac{l}{d} + 0.154 \right)} \quad (3)$$

Equation (3) predicts the Mach number at which a cavity of a given  $l/d$  will begin to oscillate in a given mode. Note the inverse relationship between this Mach number and the mode number  $n$ . Although a cavity may not oscillate below a certain Mach number in the first mode, it can oscillate at that Mach number in the higher modes. This is observed also for the cavity with  $l/d = 5.01$  in figure 4. Equation (3) predicts that for velocities up to  $M = 0.40$ , the lowest mode in which a cavity of  $l/d = 5.01$  will oscillate is  $n = 3$ . This is borne out in figure 4.

#### Strouhal Number as a Function of Length-to-Depth Ratio

The behavior of the Strouhal number as  $l/d$  varies was examined in the second phase of the experiment. The procedure for this phase has been described previously in the section entitled "Experimental Arrangement and Procedure." Figures 5 and 6 show the results of this study.

Figure 5 shows the data taken at  $M = 0.22$  for both cavity depths. The circles represent the data obtained with  $d = 3.19$  cm; the squares, with  $d = 5.11$  cm. The theory (eq. (1)), represented by the curves in figure 5, predicts an increase in Strouhal number with increasing  $l/d$ , particularly at the lower values of  $l/d$ . For  $l/d$  greater than about 3, the theory predicts that  $N_{Str}$  would be relatively insensitive to changes in  $l/d$  and this is borne out by the data. Although this ratio does enter into the calculation for  $N_{Str}$ , the dependence on  $l/d$  is weak for shallower cavities.

Figure 6 shows similarly obtained data taken at  $M = 0.35$ . Again, the theory agrees quite well with the data except for the higher modes ( $n = 5$  and  $6$ ). An explanation for the poor agreement at the higher values of  $n$  is given in reference 3. The data also show that at a given Mach number, as  $l/d$  is increased, the oscillations will jump to a higher mode. For example, at  $M = 0.35$  (fig. 6) for  $l/d \gtrsim 2$ , the cavity continues to oscillate by going from mode 1 ( $n = 1$ ) to mode 2 ( $n = 2$ ). Conversely, cavities of smaller  $l/d$  will oscillate in lower modes for a given value of  $M$ . This trend is also seen in figure 5.

These results indicate that the variation of Strouhal number with  $l/d$  is predicted by equation (1). The Strouhal number is sensitive to the  $l/d$  ratio for  $l/d \lesssim 3$  and shows that, for a given Mach number, shallower cavities tend to oscillate in the higher modes. This latter tendency is predicted by equation (3).

#### Minimum Cavity Length as a Function of Mach Number

In reference 5, Karamcheti noted that there was some minimum cavity length necessary for cavity oscillation. This minimum cavity length  $l_{\min}$  was investigated in the third phase of the experiment. The results are shown in figures 7 and 8. In these figures, the circles represent data taken with the cavity depth  $d$  at 5.11 cm, and the squares with  $d$  at 3.19 cm.

In figure 7, the minimum length is nondimensionalized by the depth and plotted against Mach number. The data were obtained by using very small increments in  $M$  to obtain a smooth continuous curve, and, in fact, the data tend to display upward trends which are interrupted by jumps or discontinuities. Thus,  $l_{\min}$  does generally increase with increasing  $M$ .

The minimum cavity length  $l_{\min}$  may also be nondimensionalized by the frequency  $f$  and the free-stream velocity  $U$  to obtain a Strouhal number,  $N_{\text{Str}} = fl_{\min}/U$ , in a manner similar to that used for figures 3 and 4. The Strouhal numbers of the data are plotted against Mach number in figure 8.

The data fall into two horizontal bands. The lower band of data has the value  $fl_{\min}/U = 0.29$ , and the second harmonic has a value of 0.58, both of which are independent of Mach number and cavity depth. This behavior also indicates a slightly different phenomenon from that which generated equation (1) or (2) and is imperfectly understood at this time.

#### CONCLUDING REMARKS

The results of a three-phase study of the tonal component of cavity noise have been presented in which the frequency of oscillation  $f$ , cavity length  $l$ , and free-stream velocity  $U$  were measured.

The Strouhal numbers  $N_{Str}$  of the data when plotted against Mach number  $M$  appear in bands which increase in slope as the Mach number decreases. For  $M \gtrsim 0.15$ , the behavior of the data is predicted by the equation developed by Block. For  $M \lesssim 0.20$ , the steep slope of some of the data is predicted by the equation developed by East, although it does not correctly predict the values of the Strouhal numbers of the data. The Mach number at which the curves described by these two equations intersect is an imprecise but useful indication of the Mach number at which cavities of a given length-to-depth ratio  $l/d$  will begin oscillation in a given mode  $n$ . The relationship for this approximate Mach number is presented herein.

The change in  $N_{Str}$  is predicted with changing  $l/d$ . For  $l/d \gtrsim 3$ ,  $N_{Str}$  is relatively insensitive to changes in  $l/d$ .

The minimum cavity length required for cavity oscillation to occur  $l_{min}$  tends to increase with Mach number although the data show many jumps or discontinuities. However, the nondimensional quantity  $fl_{min}/U$  appears to be independent of Mach number and takes on the constant values of 0.29 and 0.58.

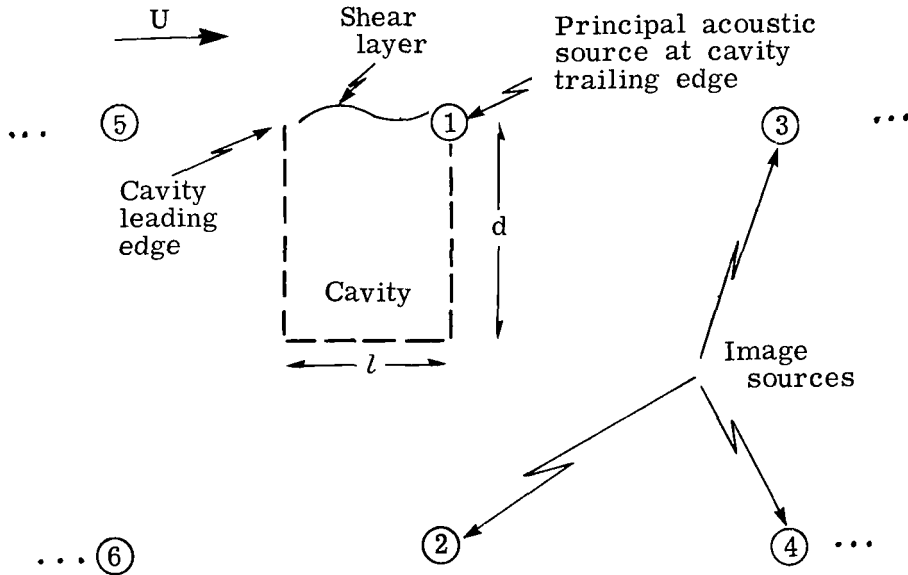
Langley Research Center  
National Aeronautics and Space Administration  
Hampton, VA 23665  
October 20, 1977

## APPENDIX A

### PREDICTION OF STROUHAL NUMBER FOR DEEPER CAVITIES

The derivation of equation (1) in the main text of this paper is presented in reference 3. This derivation may be modified so as to enhance the effect of the depthwise contribution of the sound pulses to the disturbance of the shear layer at the cavity leading edge. This approach is taken since it is known that deeper cavities tend to maintain depthwise oscillations.

The cavity is modeled in two dimensions as three hard surfaces with a thin shear layer spanning the cavity opening. The three hard surfaces are simulated mathematically through the use of acoustic images of the principal acoustic source which is located at the trailing edge of the cavity, as shown in the following sketch:



The acoustic pressure inside the cavity and, in particular, at the cavity leading edge is the sum of the acoustic fields of each of the image sources. Equation (1) was derived by assuming that the contribution at the leading edge from sources ① and ② (see sketch) was equal and much greater in effect than from any of the other sources. For deeper cavities one would expect that the contribution from source ②, which represents the bottom reflected waves from the principal source, becomes increasingly important since the depthwise oscillation is sustained. If the assumption is made that source ② is greater in effect than source ①, and greater than any of the other sources, equation (1) becomes

## APPENDIX A

$$N_{\text{Str}} = \frac{n}{\frac{1}{k_v} + M\left(0.7 + \frac{1.23}{l/d}\right)} \quad (\text{A1})$$

Equation (A1) is a modification of equation (1) for deeper cavities. It is not empirical but is based on the phase relationships within the feedback loop. For more detail, the reader is referred to the derivation in reference 3. This relation is compared with the experimental data in appendix B.

## APPENDIX B

### PRESENTATION OF RAW DATA

This appendix is provided for those interested in comparing the experimental results obtained in this study with other results or theories. The data are plotted with grids to facilitate reading the measured values. Also, for the convenience of the reader, the predictions given by equation (1) (shallow cavities) and equation (A1) (deeper cavities) are included on the graphs where appropriate.

The data from phase 1 of this experiment are given as frequency plotted against Mach number and are shown in figure 9. For deeper cavities, equation (A1) may be rewritten as

$$f = \frac{nM}{\frac{l}{ck_v} + M \frac{l}{c} \left( 0.7 + \frac{1.23}{l/d} \right)} \quad (B1)$$

Equation (B1) is plotted in figures 9(a) and 9(b) where  $l/d = 0.78$ . For shallower cavities, equation (1) may be rewritten as

$$f = \frac{nM}{\frac{l}{ck_v} + M \frac{l}{c} \left( 1 + \frac{0.514}{l/d} \right)} \quad (B2)$$

Equation (B2) is also plotted in figure 9.

The data from phase 2 are given as frequency plotted against cavity length and are shown in figure 10. Equations (B1) and (B2) are included where appropriate.

The temperature in the anechoic chamber during the recording of the data was  $20^{\circ} \pm 1.7^{\circ}$  C. The speed of sound  $c$  used to calculate the Mach number was 343 m/s. The temperature variation resulted in a maximum error in the Mach number calculation ( $M = U/c$ ) of  $\pm 0.3$  percent.

## REFERENCES

1. Block, Patricia J. W.; and Heller, H. Hanno: Measurements of Farfield Sound Generation From a Flow-Excited Cavity. NASA TM X-3292, 1975.
2. Rossiter, J. E.: Wind Tunnel Experiment on the Flow Over Rectangular Cavities at Subsonic and Transonic Speeds. R. & M. No. 3438, British A.R.C., Oct. 1964.
3. Block, Patricia J. W.: Noise Response of Cavities of Varying Dimensions at Subsonic Speeds. NASA TN D-8351, 1976.
4. Bilanin, Alan J.; and Covert, Eugene E.: Estimation of Possible Excitation Frequencies for Shallow Rectangular Cavities. AIAA J., vol. 11, no. 3, Mar. 1973, pp. 347-351.
5. Krishnamurty, K.: Acoustic Radiation From Two-Dimensional Rectangular Cutouts in Aerodynamic Surfaces. NACA TN 3487, 1955.
6. Block, P. J. W.: An Experimental Investigation of Airframe Component Interference Noise. AIAA Paper No. 77-56, Jan. 1977.
7. East, L. F.: Aerodynamically Induced Resonance in Rectangular Cavities. J. Sound & Vib., vol. 3, no. 3, May 1966, pp. 277-287.

TABLE I.- CAVITY DIMENSIONS USED IN FIRST PHASE  
OF EXPERIMENT

$l$ , cm	$w$ , cm	$d$ , cm	$l/d$
4	5.08	5.11	0.78
2.5	↓	3.19	.78
12		5.11	2.35
7.5		3.19	2.35
16.0		3.19	5.01



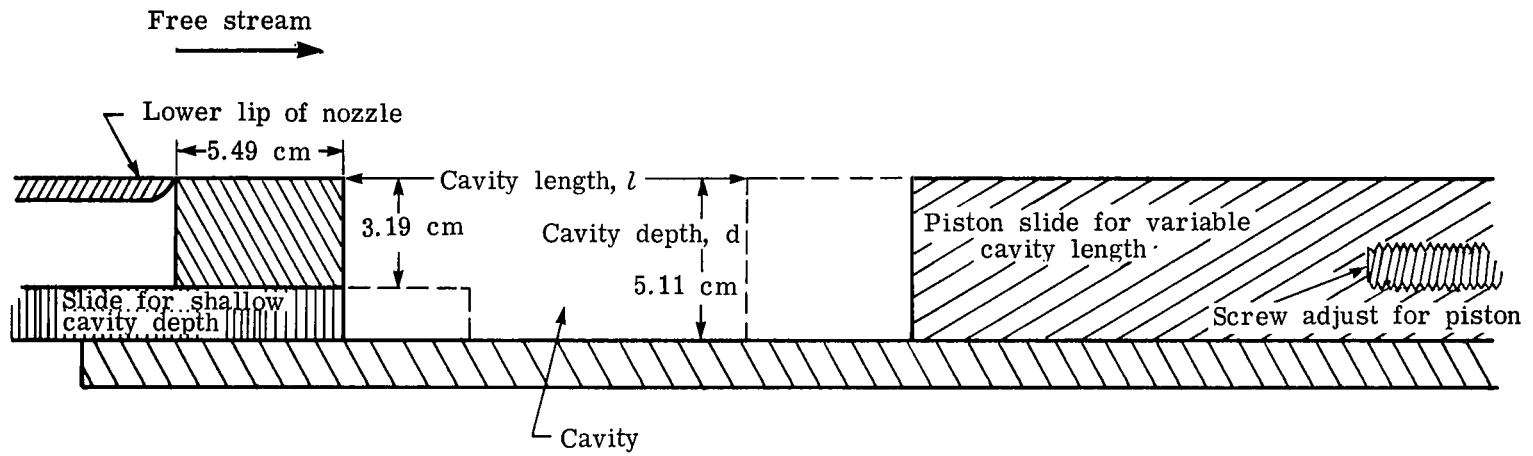


Figure 1. - Cross-sectional view of cavity.

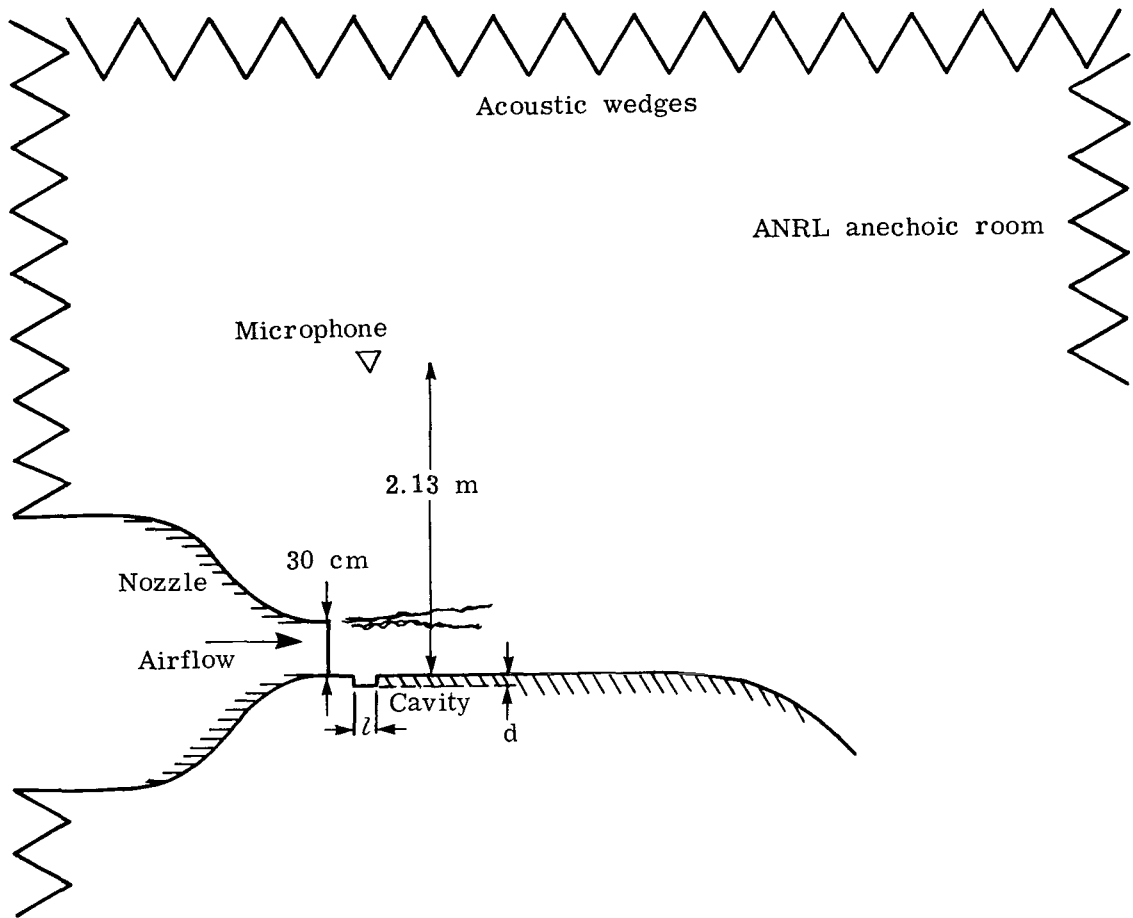


Figure 2.- Schematic drawing of cavity apparatus in ANRL open-jet anechoic flow facility.

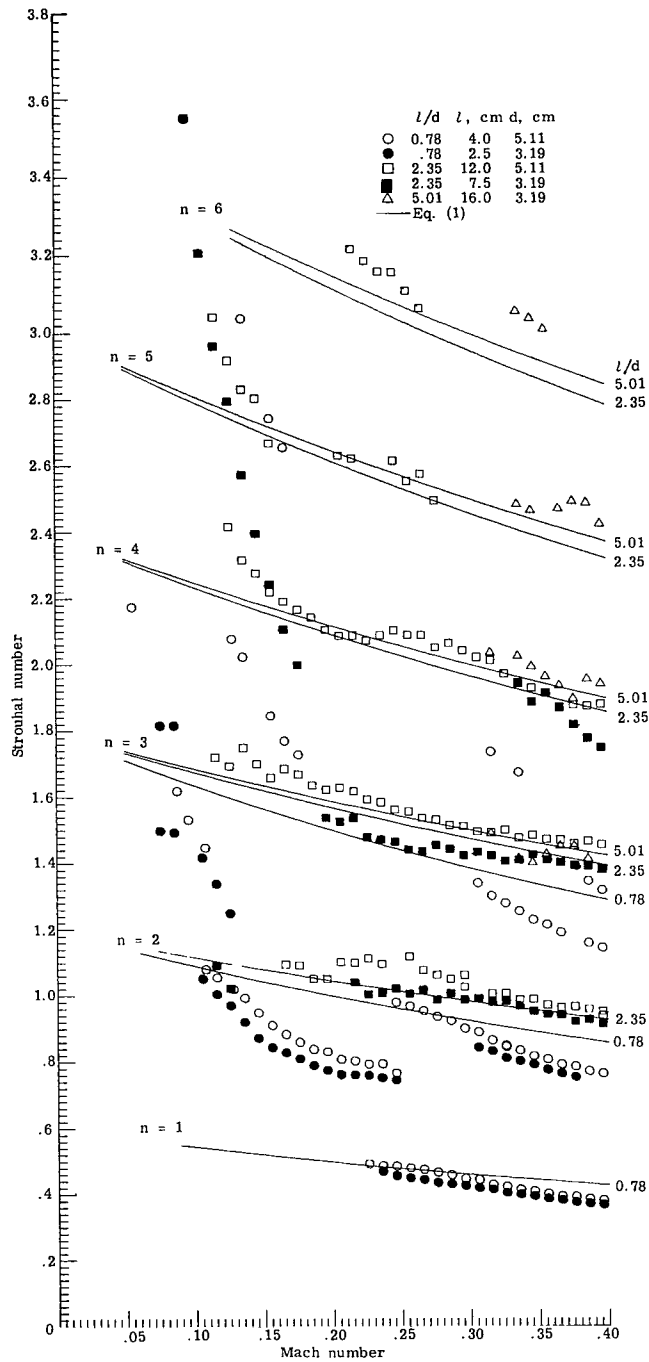


Figure 3.- Comparison of data with prediction of equation (1).

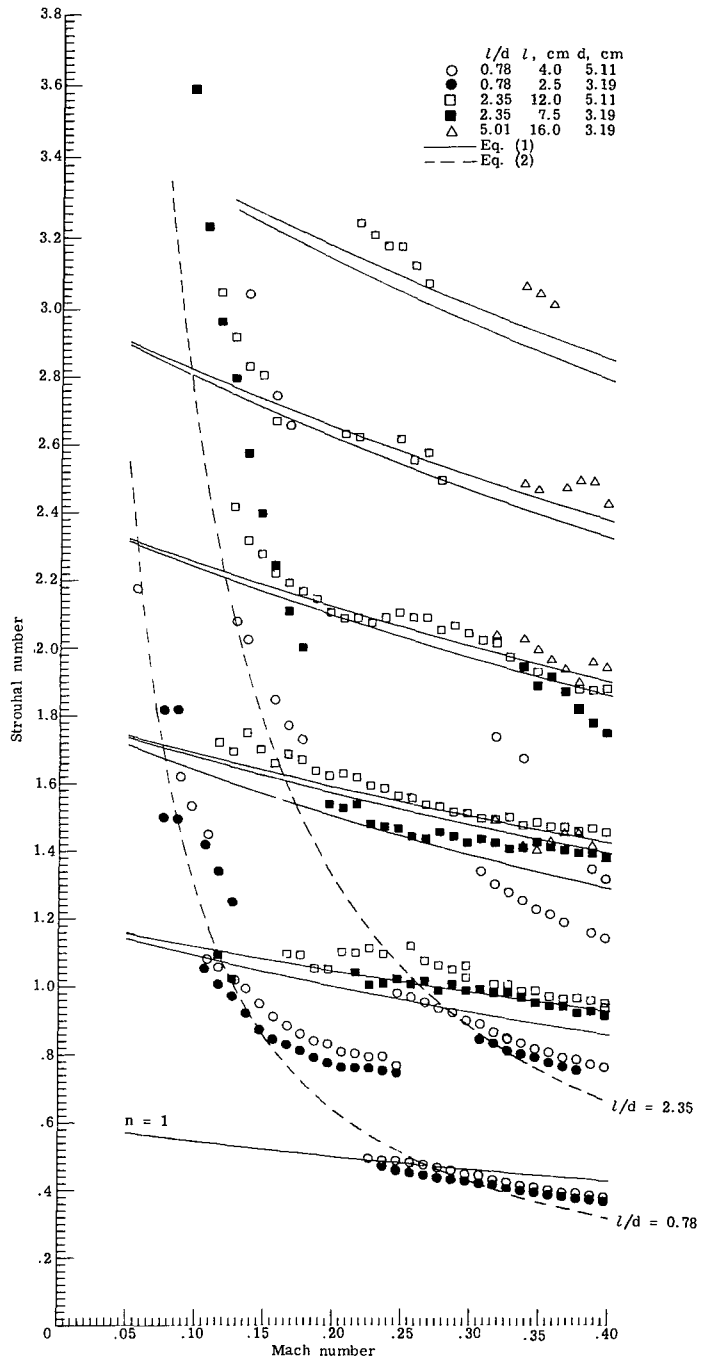


Figure 4. - Comparison of data with equations (1) and (2).

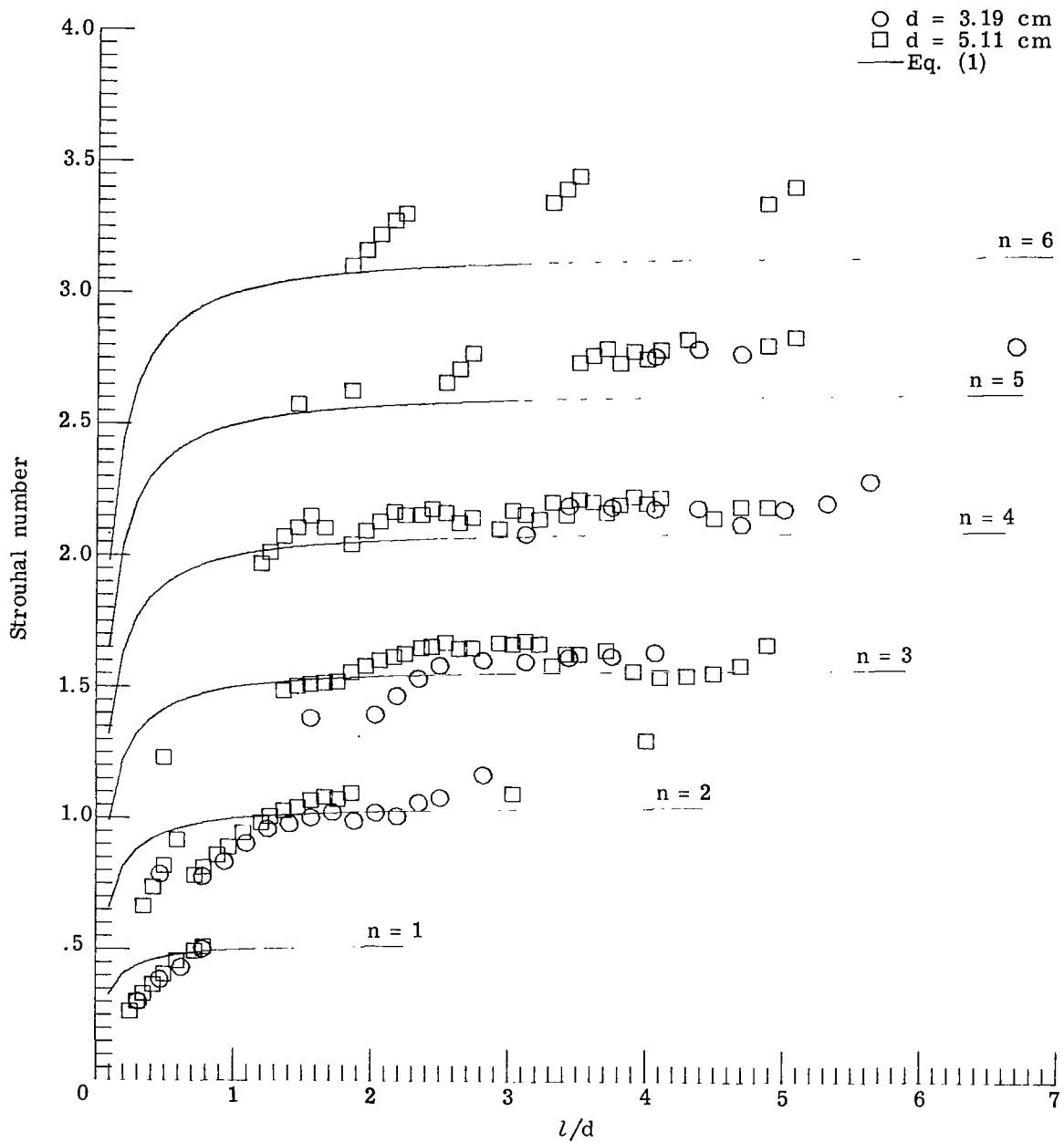


Figure 5.- Comparison of experiment with theory at  $M = 0.22$ .

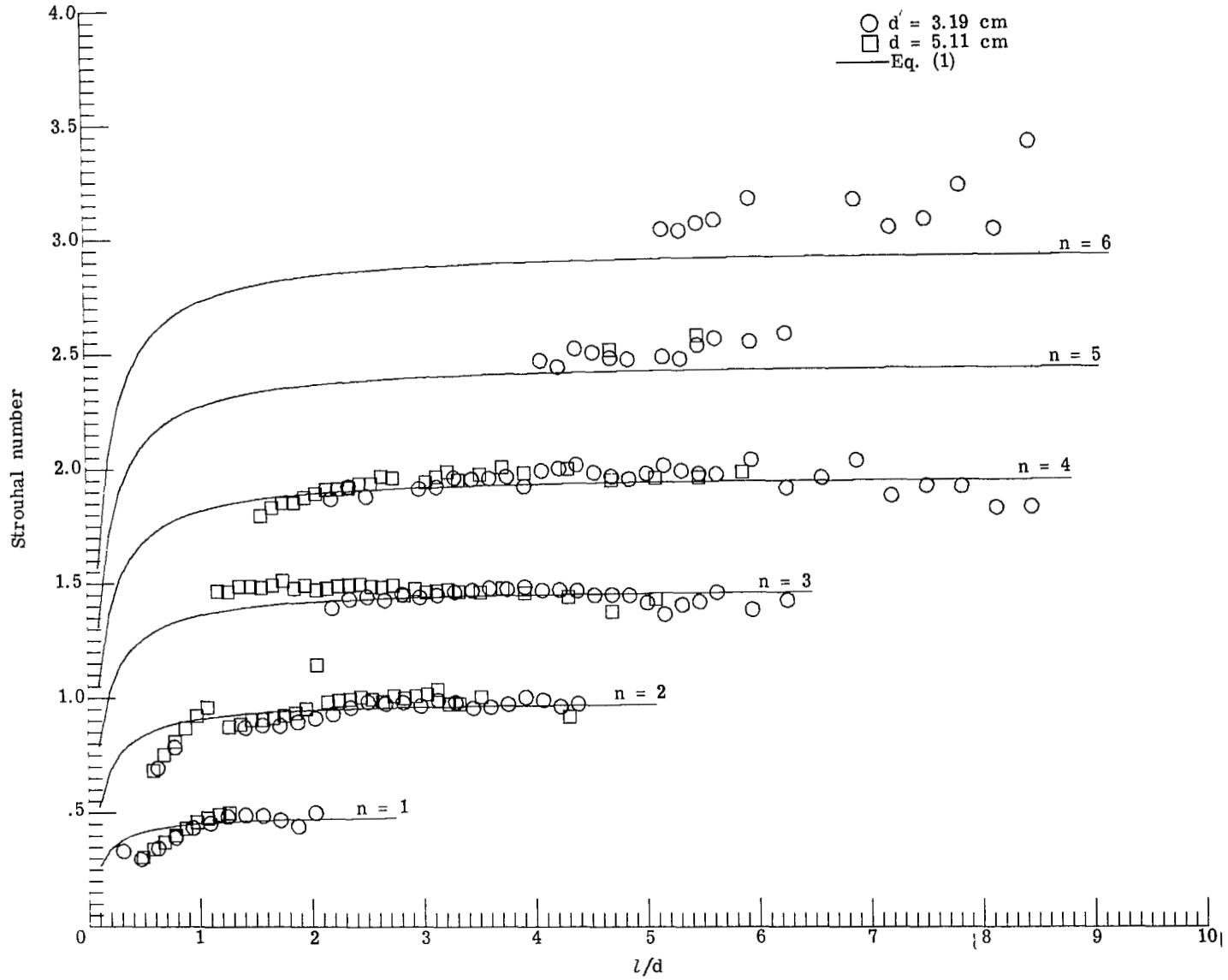


Figure 6.- Comparison of experiment with theory at  $M = 0.35$ .

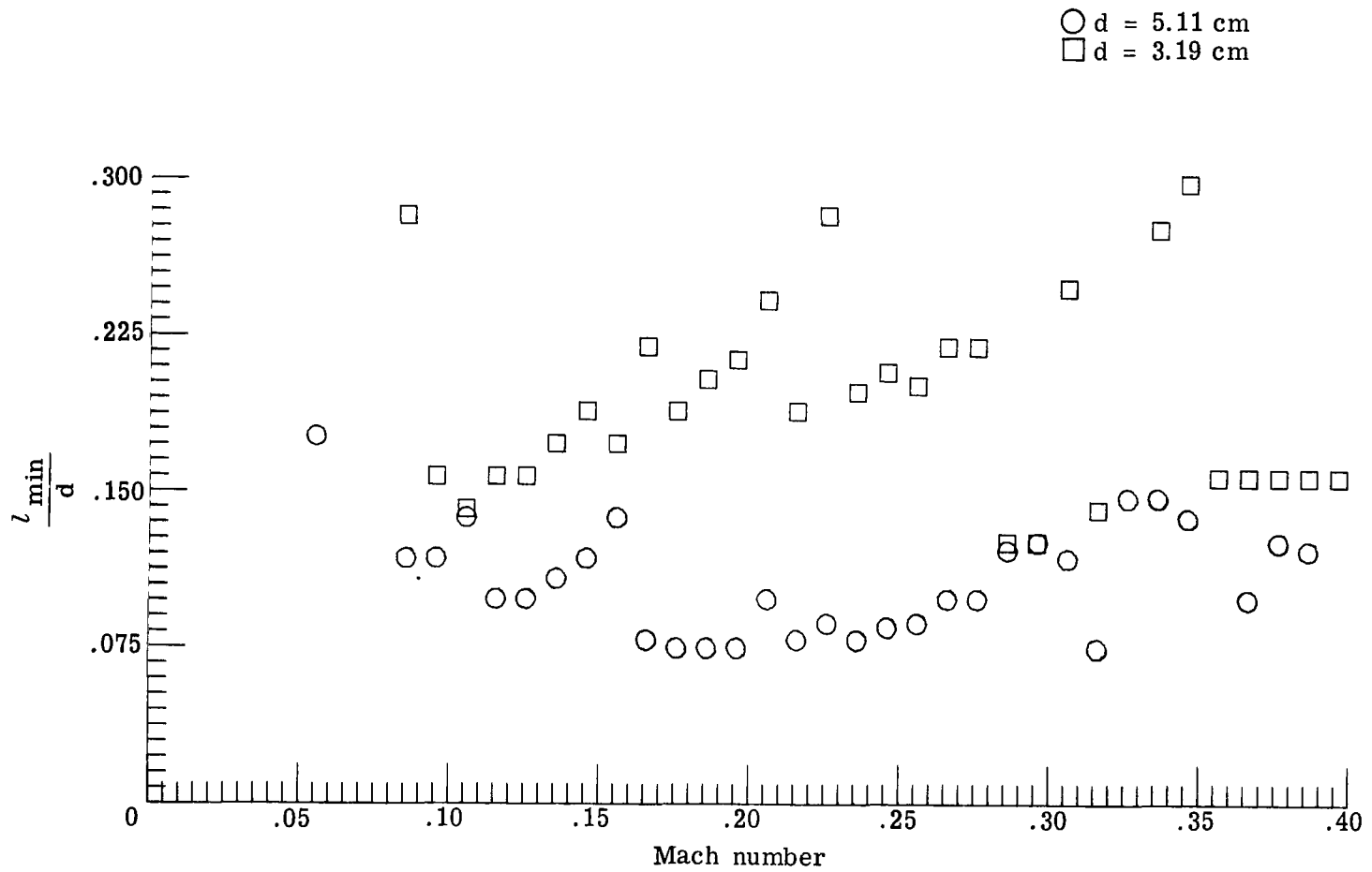


Figure 7.- Minimum cavity length required for oscillation as a function of Mach number.

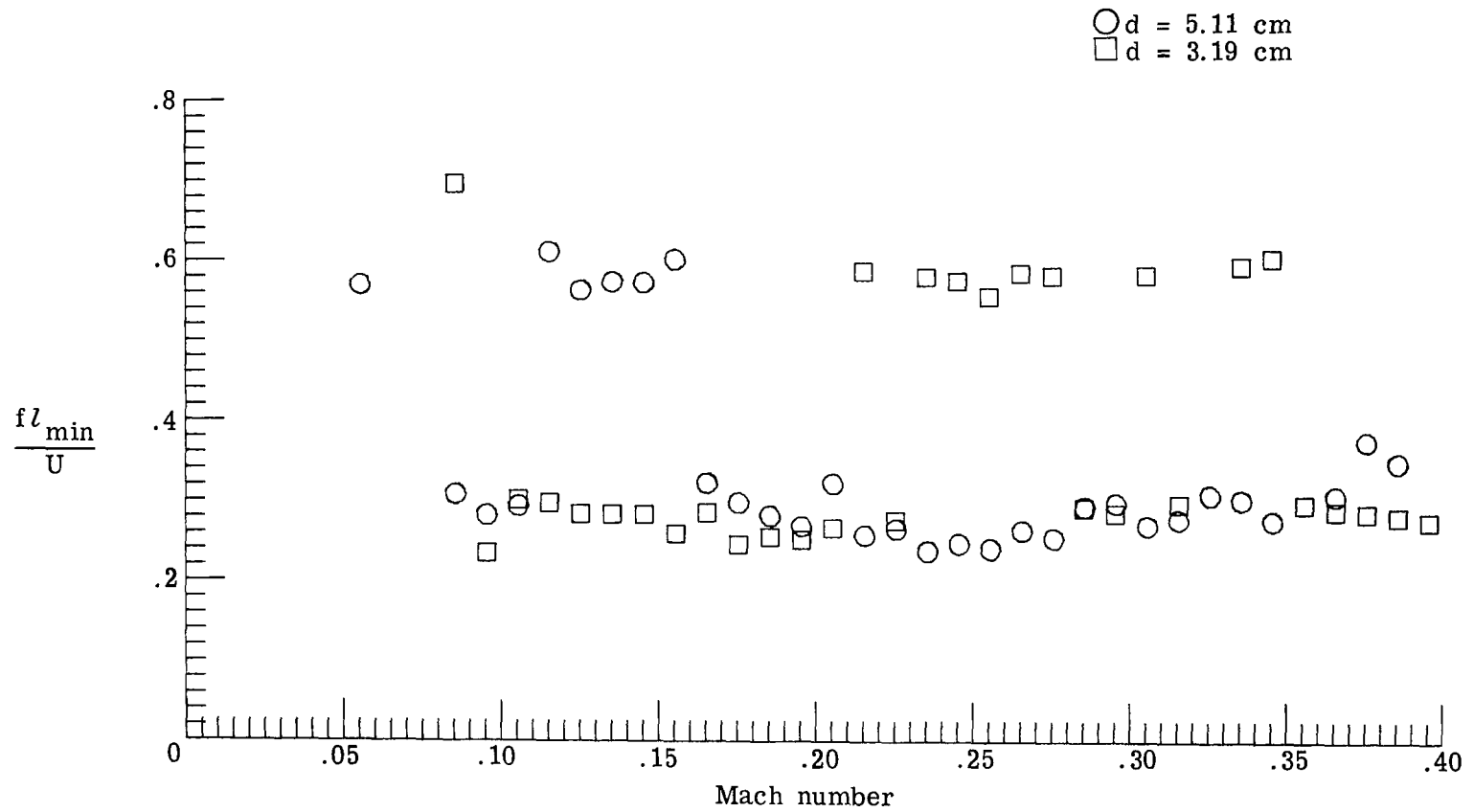
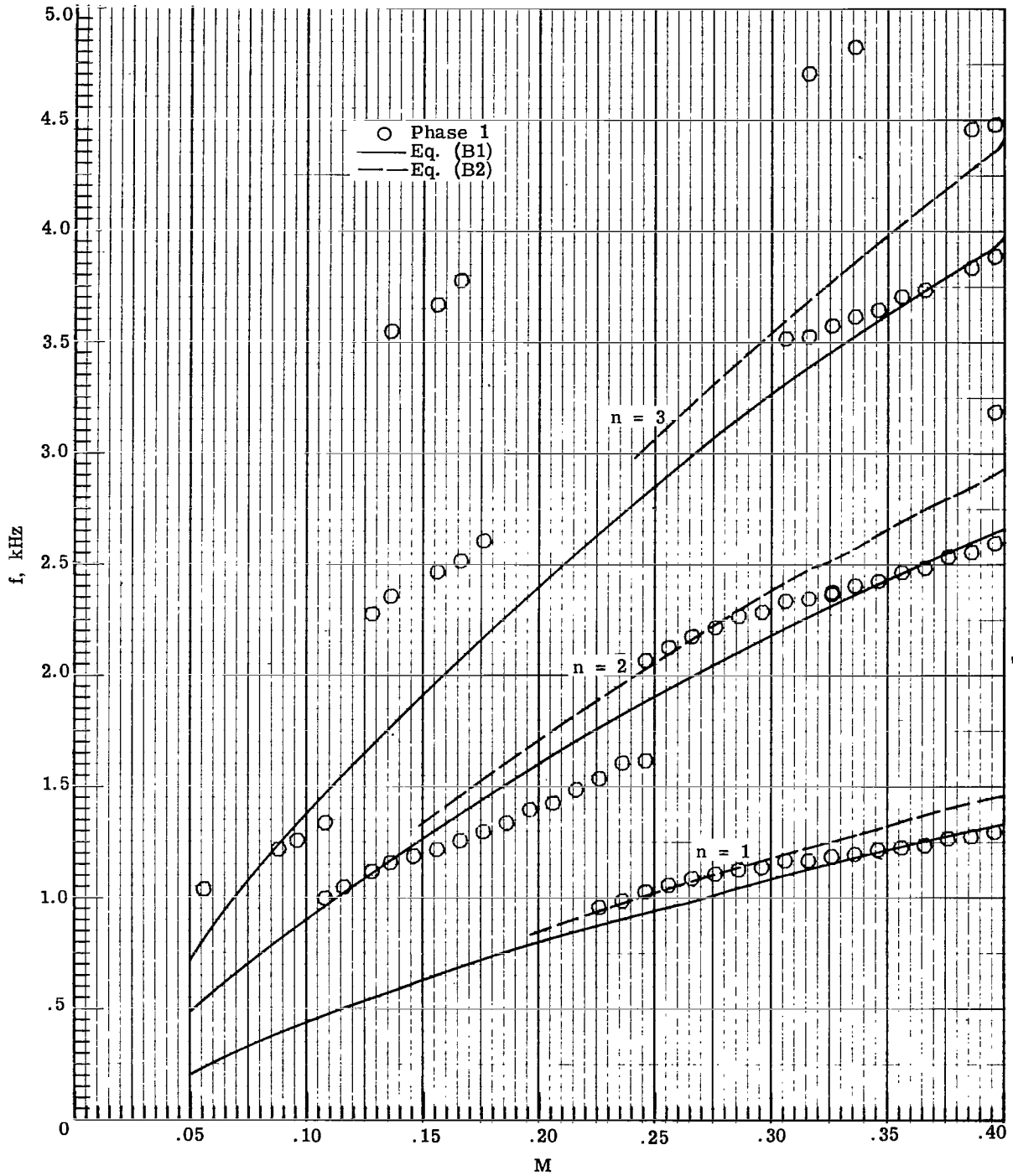


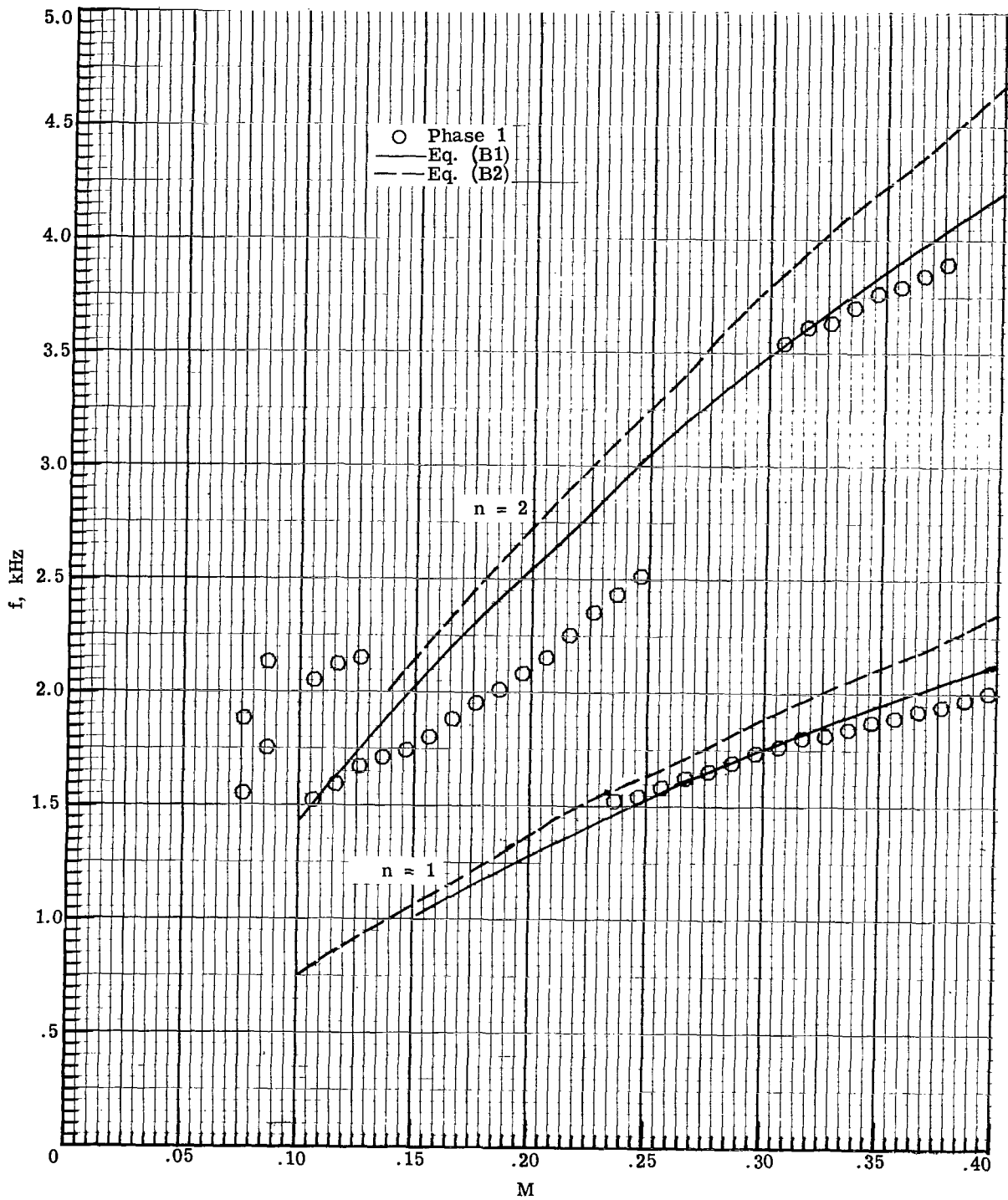
Figure 8.- Strouhal number based on minimum cavity length.





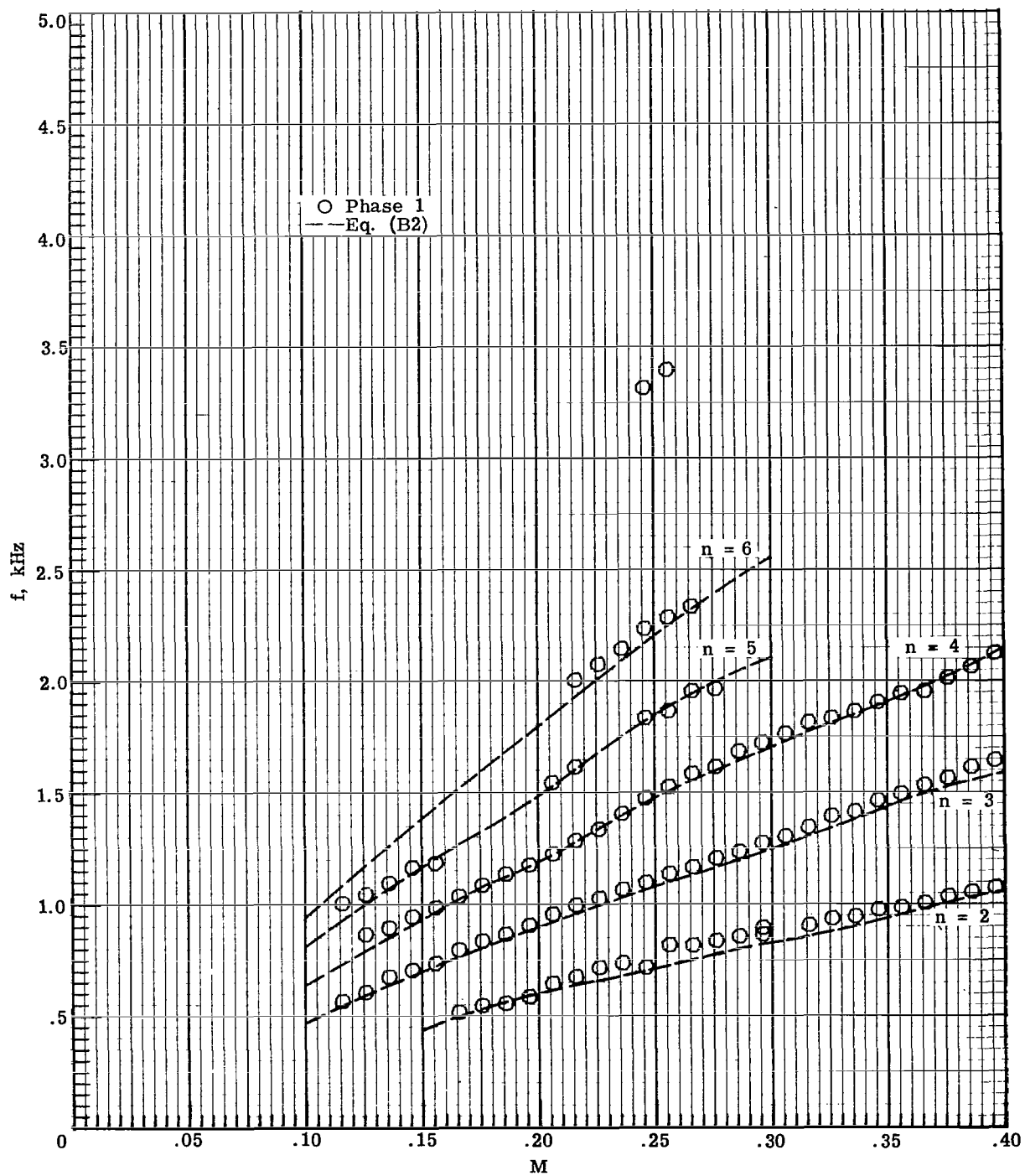
(a)  $l = 4$  cm;  $l/d = 0.78$ .

Figure 9.- Cavity-oscillation frequency plotted against Mach number of data from phase 1.



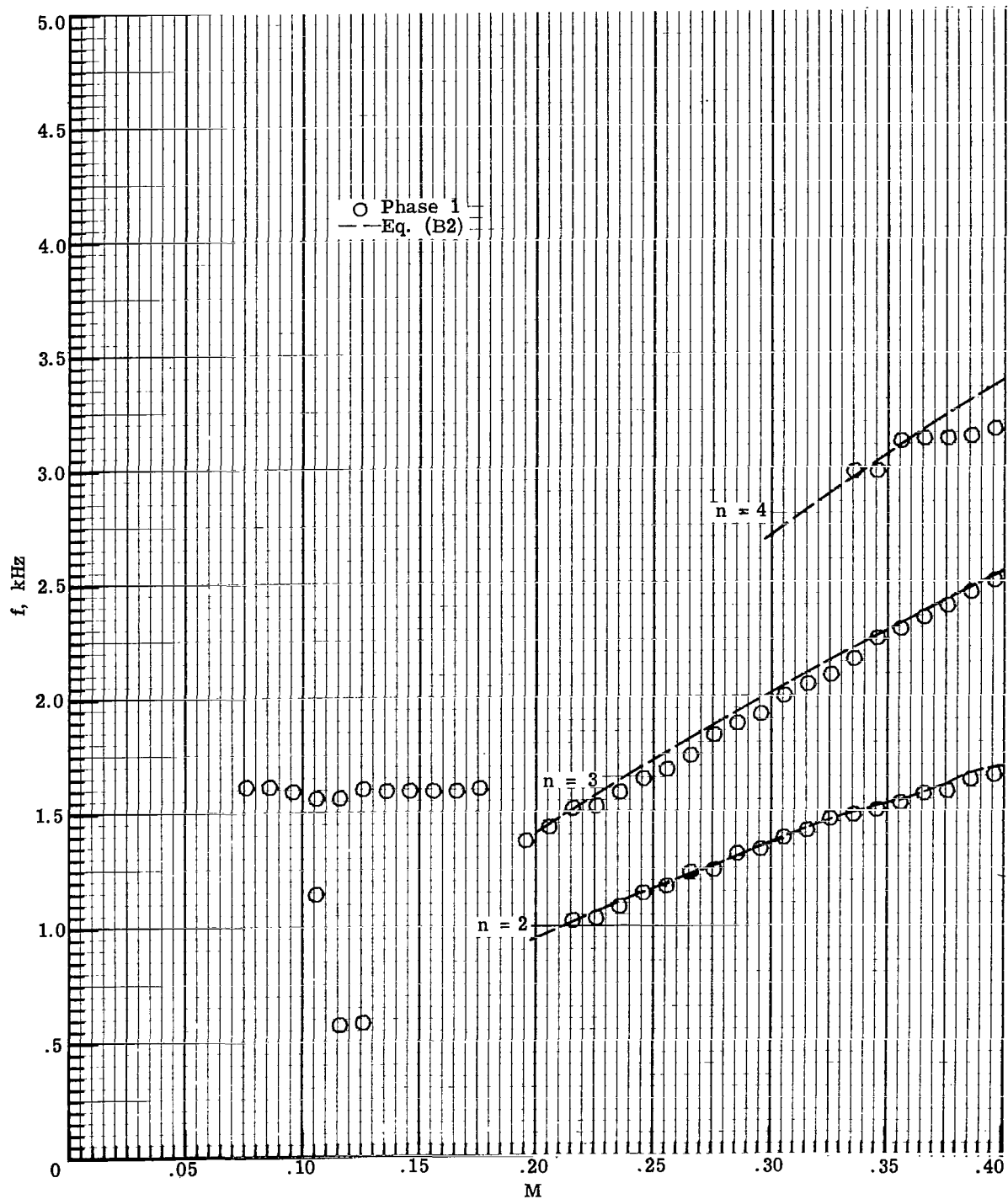
(b)  $l = 2.5$  cm;  $l/d = 0.78$ .

Figure 9. - Continued.



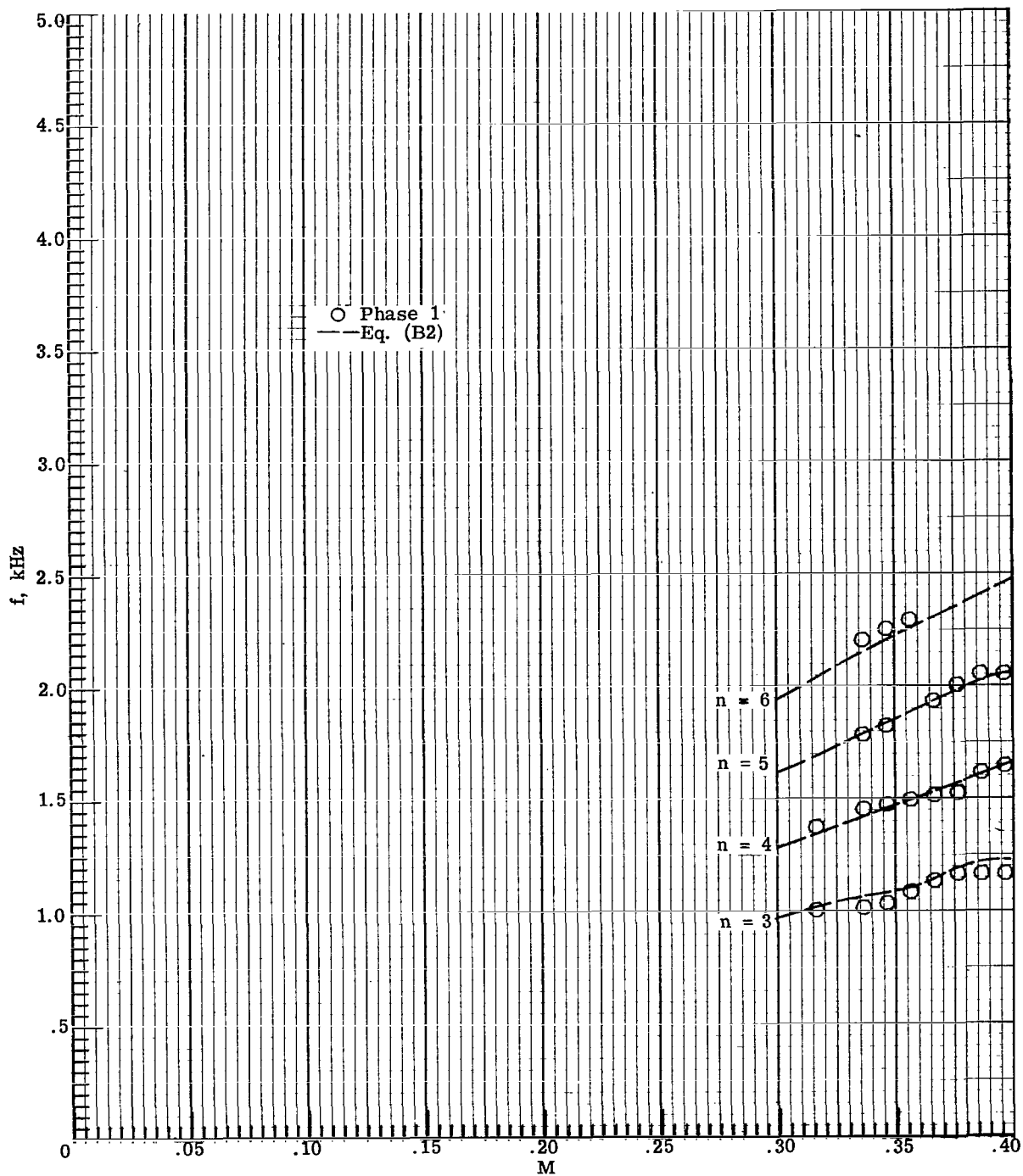
(c)  $l = 12$  cm;  $l/d = 2.35$ .

Figure 9. - Continued.



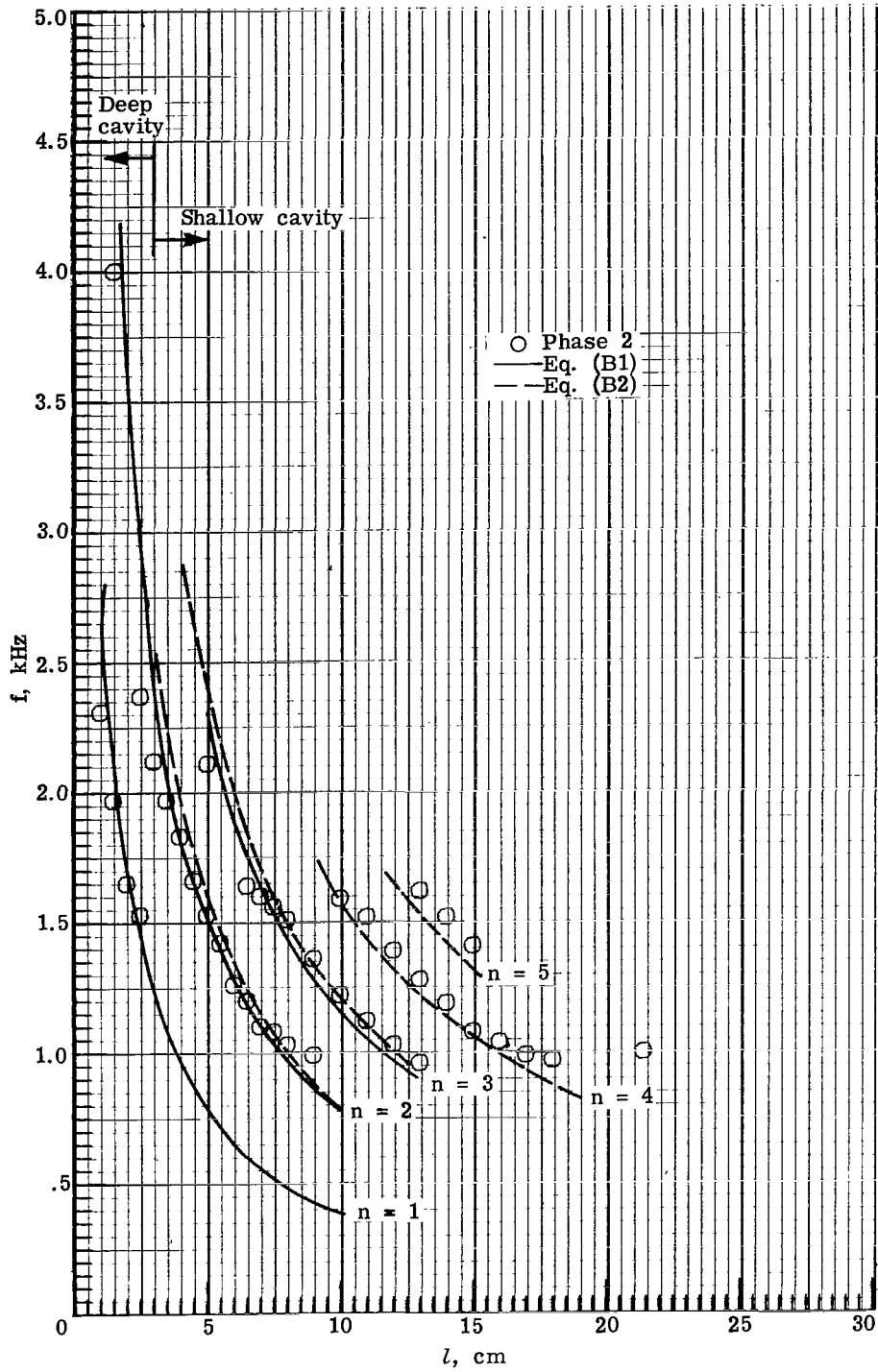
(d)  $l = 7.5 \text{ cm}$ ;  $l/d = 2.35$ .

Figure 9. - Continued.



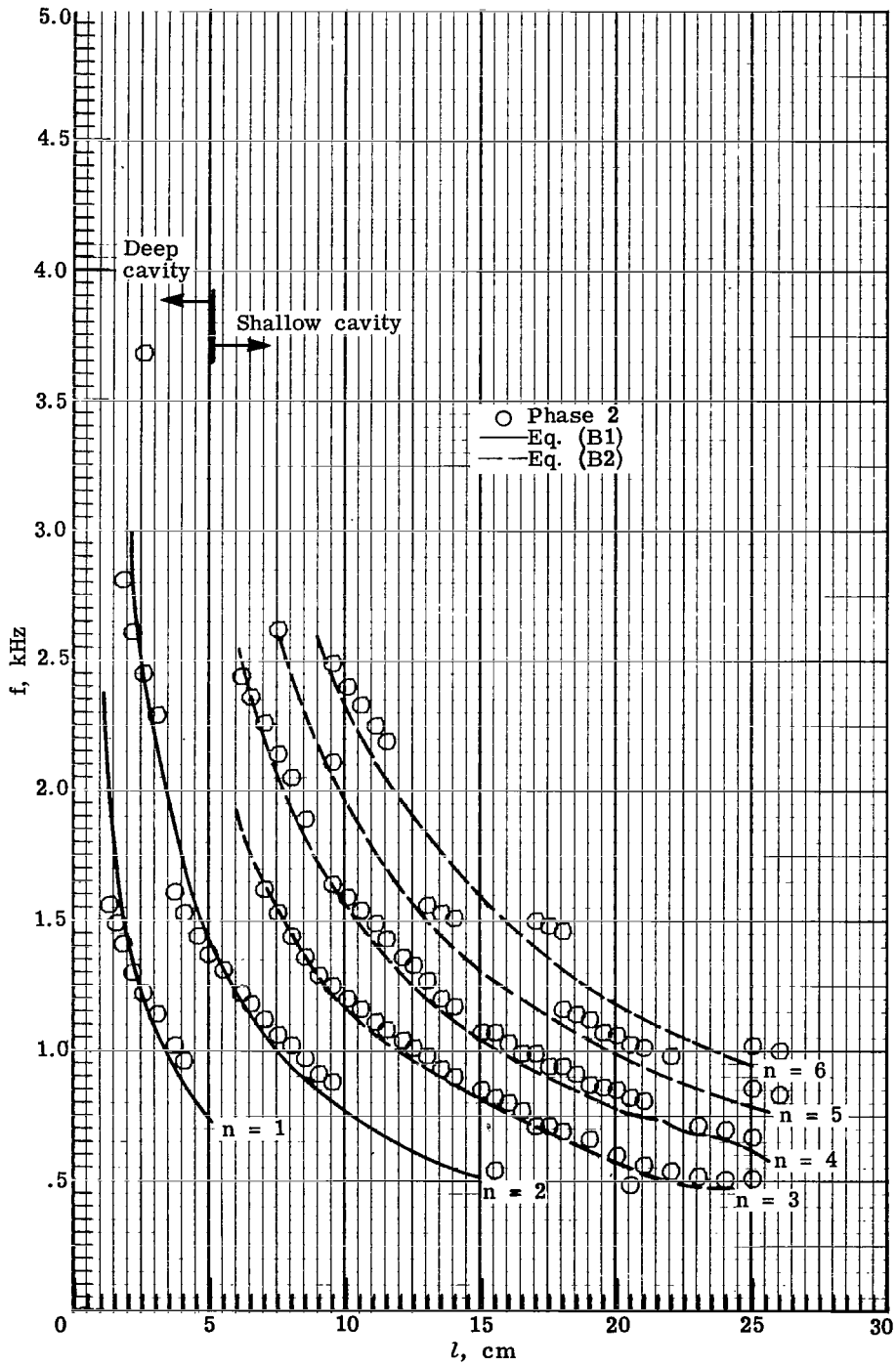
(e)  $l = 16$  cm;  $l/d = 5.01$ .

Figure 9.- Concluded.



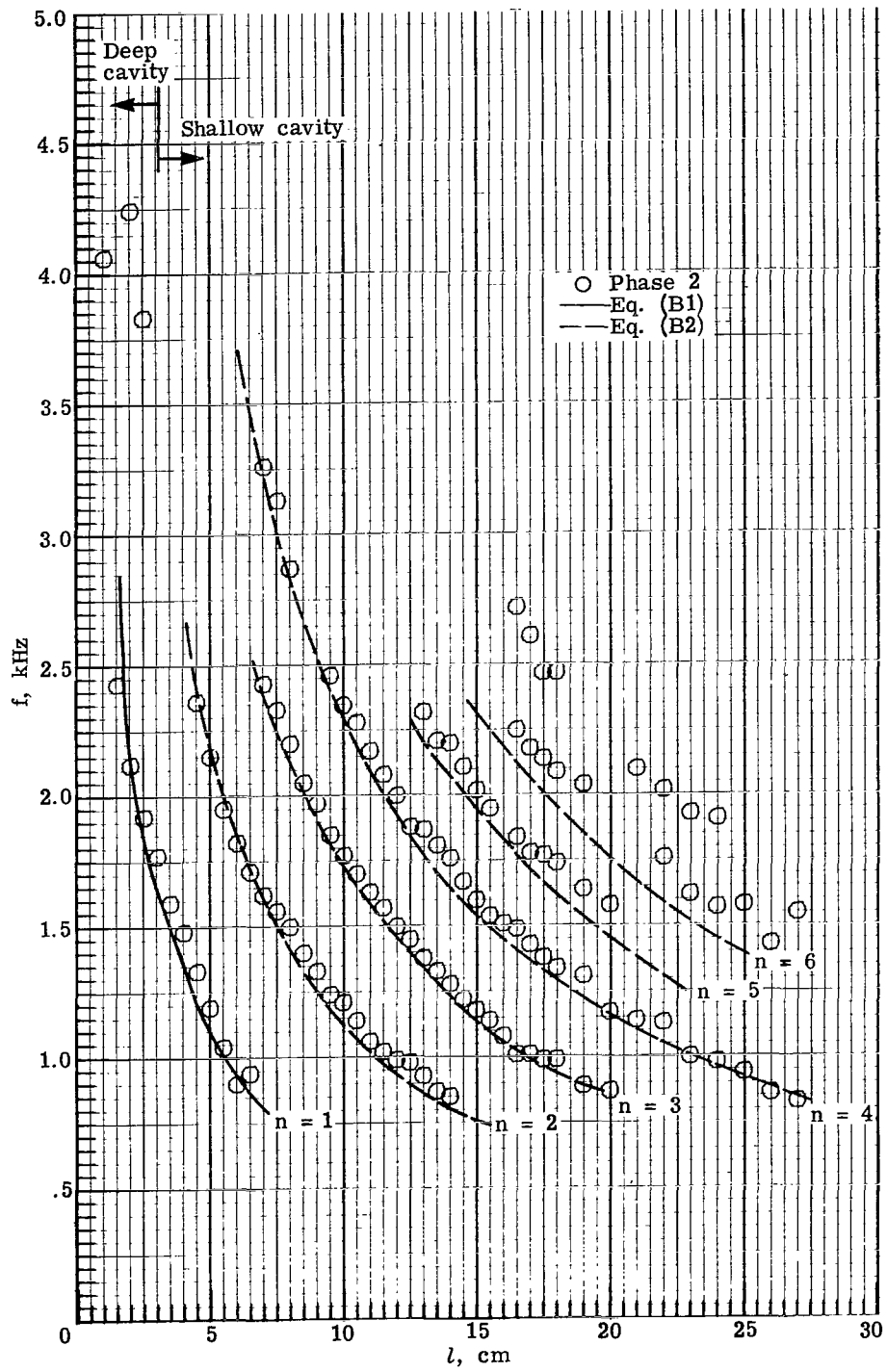
(a)  $M = 0.22$ ;  $d = 3.19$  cm.

Figure 10.- Cavity-oscillation frequency plotted against cavity length of data from phase 2.



(b)  $M = 0.22$ ;  $d = 5.11$  cm.

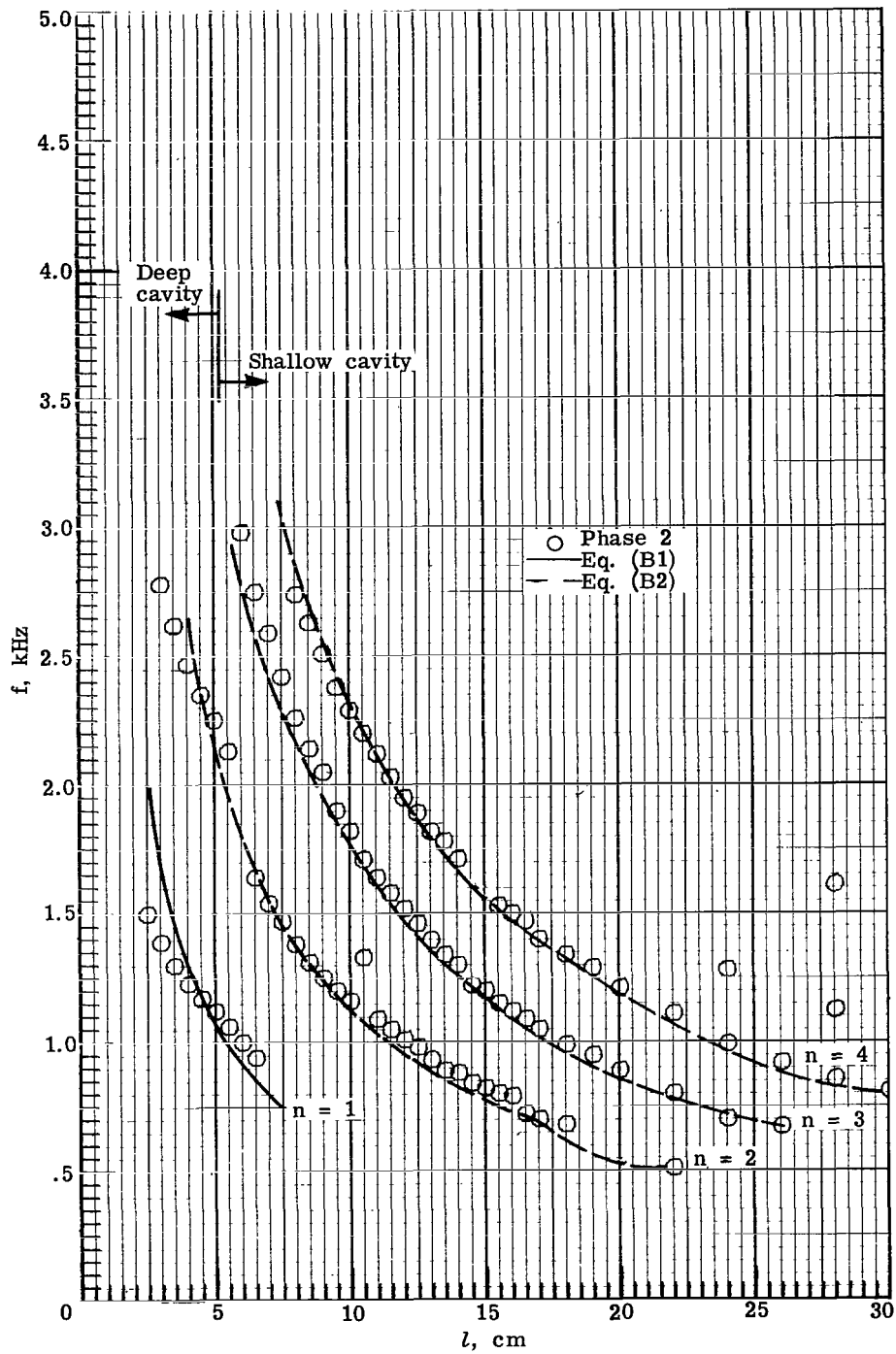
Figure 10.- Continued.



(c)  $M = 0.35$ ;  $d = 3.19$  cm.

Figure 10.- Continued.





(d)  $M = 0.35$ ;  $d = 5.11$  cm.

Figure 10. - Concluded.

1. Report No. NASA TP-1013		2. Government Accession No.		3. Recipient's Catalog No.	
4. Title and Subtitle MEASUREMENTS OF THE TONAL COMPONENT OF CAVITY NOISE AND COMPARISON WITH THEORY				5. Report Date November 1977	
				6. Performing Organization Code	
7. Author(s) P. J. W. Block				8. Performing Organization Report No. L-11620	
9. Performing Organization Name and Address NASA Langley Research Center Hampton, VA 23665				10. Work Unit No. 505-06-23-01	
				11. Contract or Grant No.	
12. Sponsoring Agency Name and Address National Aeronautics and Space Administration Washington, DC 20546				13. Type of Report and Period Covered Technical Paper	
				14. Sponsoring Agency Code	
15. Supplementary Notes					
16. Abstract  This paper presents the results of a detailed study of the frequency of the tonal noise generated by a flow-excited rectangular cavity. The Mach number in this experimental study ranged from 0.05 to 0.40, and the cavity length-to-depth ratio varied from 0.1 to 8. The data are used to evaluate a current prediction method and good agreement is shown. Measurements of the minimum streamwise cavity length required for oscillation were also made.					
17. Key Words (Suggested by Author(s))  Cavity noise Noise Aerodynamic sound			18. Distribution Statement  Unclassified - Unlimited  Subject Category 71		
19. Security Classif. (of this report) Unclassified		20. Security Classif. (of this page) Unclassified		21. No. of Pages 31	22. Price* \$ 4.00

\* For sale by the National Technical Information Service, Springfield, Virginia 22161

National Aeronautics and  
Space Administration

Washington, D.C.  
20546

Official Business

Penalty for Private Use, \$300

THIRD-CLASS BULK RATE

Postage and Fees Paid  
National Aeronautics and  
Space Administration  
NASA-451



5 1 1U,H. 102777 S00903DS  
DEPT OF THE AIR FORCE  
AF WEAPONS LABORATORY  
ATTN: TECHNICAL LIBRARY (SUL)  
KIRTLAND AFB NM 87117

**NASA**

---

POSTMASTER: If Undeliverable (Section 158  
Postal Manual) Do Not Return